

Marine and Petroleum Geology

Back-arc underplating provided crustal accretion affecting topography and sedimentation in the Adria microplate

--Manuscript Draft--

Manuscript Number:	JMPG-D-21-00861R1
Article Type:	Full Length Article
Keywords:	Underplating; Crustal Accretion; Magnetic Anomalies; Adria Plate
Corresponding Author:	Paolo Mancinelli, Ph.D. Universita degli Studi Gabriele d'Annunzio Chieti Pescara Chieti, ITALY
First Author:	Paolo Mancinelli, Ph.D.
Order of Authors:	Paolo Mancinelli, Ph.D. Vittorio Scisciani Cristina Pauselli Gérard M. Stampfli Fabio Speranza Ivana Vasiljevic
Abstract:	Supported by evidence of deep crustal sources for the observed magnetic anomalies in Central Italy and by outcropping gabbros in the Croatian archipelago, we model the observed gravity and magnetic anomalies in the Central Adriatic Sea and surroundings. We suggest that the major magnetic anomalies in the area are related to a wide underplating and propose that this volume represents the first stage of the back-arc Adria continental breakup in Early Permian times. During the Palaeotethys-Adria collision, underplating has controlled topography and palaeogeographic domains resulting in the observed asymmetrical sedimentary evolution since the Triassic across the Adria microplate. Finally, we propose that the Palaeotethys-Adria boundary in the Early Permian was similar to the current Pacific-Okhotsk plate boundary.

Highlights for the manuscript

“Back-arc underplating provides crustal accretion affecting topography and sedimentation”

Paolo Mancinelli^{1*}, Vittorio Scisciani¹, Cristina Pauselli², Gérard M. Stampfli³, Fabio Speranza⁴, Ivana Vasiljević⁵

* Corresponding author: paolo.mancinelli@unich.it ORCID: 0000-0003-4524-3199

¹ Dipartimento di Ingegneria e Geologia, Università G. D’Annunzio di Chieti-Pescara.

² Dipartimento di Fisica e Geologia, Università degli Studi di Perugia

³ Institute of Earth Sciences, Université de Lausanne

⁴ Istituto Nazionale di Geofisica e Vulcanologia, Roma

⁵ Faculty of Mining and Geology, University of Belgrade

Highlights:

- We model gravity and magnetic anomaly across Apennines, Adriatic Sea and Dinarides
- The main magnetic anomalies are related to a wide Early Permian underplating event
- Underplating controlled topography, palaeogeography and sedimentary domains
- Palaeotethys-Adria boundary was similar to the current Pacific-Okhotsk boundary
- Magmatic underplating related to plates collision provides crustal accretion

1 **Back-arc underplating provided crustal accretion affecting topography and** 2 **sedimentation in the Adria microplate**

3
4
5 3 Paolo Mancinelli^{1*}, Vittorio Scisciani¹, Cristina Pauselli², Gérard M. Stampfli³, Fabio Speranza⁴, Ivana
6
7 4 Vasiljević⁵
8

9 5 * Corresponding author: paolo.mancinelli@unich.it ORCID: 0000-0003-4524-3199

10 6 ¹ Dipartimento di Ingegneria e Geologia, Università G. D'Annunzio di Chieti-Pescara.

11 7 ² Dipartimento di Fisica e Geologia, Università degli Studi di Perugia

12 8 ³ Institute of Earth Sciences, Université de Lausanne

13 9 ⁴ Istituto Nazionale di Geofisica e Vulcanologia, Roma

14 10 ⁵ Faculty of Mining and Geology, University of Belgrade
15
16
17

18 **Keywords**

19 12 Underplating; Crustal Accretion; Magnetic Anomalies; Adria Plate
20
21
22
23
24
25

26 **Abstract**

27
28
29 16 Supported by evidence of deep crustal sources for the observed magnetic anomalies in Central Italy and by
30
31 17 outcropping gabbros in the Croatian archipelago, we model the observed gravity and magnetic anomalies
32
33 18 in the Central Adriatic Sea and surroundings. We suggest that the major magnetic anomalies in the area are
34
35 19 related to a wide underplating and propose that this volume represents the first stage of the back-arc Adria
36
37 20 continental breakup in Early Permian times. During the Palaeotethys-Adria collision, underplating has
38
39 21 controlled topography and palaeogeographic domains resulting in the observed asymmetrical sedimentary
40
41 22 evolution since the Triassic across the Adria microplate. Finally, we propose that the Palaeotethys-Adria
42
43 23 boundary in the Early Permian was similar to the current Pacific-Okhotsk plate boundary.
44
45
46
47
48
49
50
51
52
53
54
55
56
57
58
59
60
61
62
63
64
65

26 **Introduction**

1
2
3
4
5
6
7
8
9
10
11
12
13
14
15
16
17
18
19
20
21
22
23
24
25
26
27
28
29
30
31
32
33
34
35
36
37
38
39
40
41
42
43
44
45
46
47
48
49
50
51
52
53
54
55
56
57
58
59
60
61
62
63
64
65

Magmatic underplating in crustal formation and evolution is often related to plate tectonic and dynamic processes. Though underplating is very common in extensional settings where it is associated to crustal breakup, this process is also responsible for large-scale flood basalt volcanic districts. Conversely, in collisional and subduction settings the role of underplated volumes is less obvious and the effects on crustal accretion in the back-arc area are still questioned. Traditionally, the distinctive features of magmatic underplating are high seismic P- and S-wave velocities and high ratio of P- to S-wave velocities of the intruded volume compared to surrounding crust (Thybo and Artemieva, 2013). More general, the products and crustal structures derived from underplating processes may range in a wide spectra, mostly depending on the geodynamic setting. Thus, if the crustal thermal state is favorable, magnetic anomalies can be included among the features diagnostic of magmatic underplating (e.g. Bronner et al., 2011).

The Adria plate today extends along the Adriatic Sea from the Po plain to the Apulian promontory and is surrounded by the Alpine, Dinaride-Albanide and Apenninic orogens to the north, east and west, respectively (Figure 1a). Seismic and GPS evidence suggests that the Adria plate is fragmented at present in two microplates, the Adria *sensu stricto* (s.str.) to the north and the Apulia s.str. to the south (Oldow et al., 2002; D'Agostino et al., 2008; Handy et al., 2019) but whether this division has developed in recent times or whether it was inherited from older geological epochs is unclear. Mesozoic and Cenozoic evolution of the Adria plate is related to a wider geodynamic setting involving the African and the Eurasian Plates whose relative motions allowed the observed counterclockwise rotation of the plate since the Cretaceous (Bennett et al., 2008; Faccenna et al., 2014). In Permian times this area was located in the northernmost pivot of the Palaeotethys, in a region supposed to have undergone transcurrent deformation (e.g. Molli et al., 2020) and wide continental extension related to the subduction and slab roll-back of the Palaeotethys ocean and, during Late Permian and Triassic, of the Neotethys to the west (Moix et al., 2008; Stampfli and Hochard, 2009; Stampfli et al., 2013). To date however, evidence of the ancient Adria s.str. oceanic crust are missing across the entire plate from the Dinarides to the Apennines (Sun et al., 2019; van Unen et al., 2019).

52 Despite the current tight setting, locations of the boundaries between the Adria plate and the surrounding
1
253 plates are still matter of debate (Anderson and Jackson, 1987; Stein and Sella, 2005; Stampfli and Hochard,
3
4
54 2009), whereby several authors (Herak, 1986; Moretti and Royden, 1988; Doglioni et al., 1994; Tari, 2002;
5
6
755 Bennett et al., 2008; Korbar, 2009; Faccenna et al., 2014; Mancinelli et al., 2018; Sun et al., 2019) suggest
8
956 that the Adria is subducting both beneath the Dinaric and the Apenninic belts. The Central Adriatic Sea is
10
11
1257 geographically surrounded by remnants of Permian and Triassic volcanism that is outcropping or has been
13
1458 drilled by explorative boreholes. These products are related to two distinguished major episodes, on one
15
1659 side there is evidence of scattered extension-related volcanism between Late Permian and Middle Triassic
17
18
1960 in the Alps, Po Plain, Northern Adriatic, Istria Peninsula, Dinarides and Apulian Peninsula (e.g. Buser, 1987;
20
2161 Tari, 2002; Velić et al, 2002; Pamić and Balen, 2005; Bernoulli, 2007; Cassinis et al., 2008; Schuster and
22
23
2462 Stüwe, 2008; Gaetani, 2010; Scisciani and Esetime, 2017; Molli et al., 2020), while in the Southern Alps
25
2663 there is evidence of wide intrusive and effusive bodies that some authors interpret as related to the
27
2864 subduction of the Palaeotethys ocean beneath Eurasia in Permian times (Cassinis et al., 2012). Moreover, a
29
30
3165 Permian underplating event was associated with post-Hercynian outcrops across the European Alps
32
3366 (Schuster and Stüwe, 2008). For a compelling review of the pre-Mesozoic exposures in the Italian peninsula
34
35
3667 and surroundings the reader is referred to the recent work by Molli et al. (2020 and references therein).
37
38
3968 Some clues about the early history of the Adria plate are preserved in the Croatian archipelago where
40
4169 gabbroic intrusions are found on the Jabuka and Brusnik islets (Balogh et al., 1994; Juračić et al., 2004;
42
4370 Pamić and Balen, 2005; Palinkaš et al., 2010). Targeted by several datings during the years, the estimated
44
45
4671 age of these gabbroic intrusions ranges between 200 and 273 ± 1.1 Ma with latter Ar/Ar dating (Palinkaš et
47
4872 al., 2010) supporting the older age together with later reworking of the gabbros of Jabuka at 77 ± 2.4 Ma.
49
50
5173 Two main questions arise from these outcrops in the Croatian archipelago: are they representative of some
52
53
5474 larger-scale event? Can these gabbroic intrusions tell us something about the pre-Mesozoic history of the
55
5675 Adria plate?
57
58
5976 Several authors attempted in the last years to answer these questions through several efforts focused on
60
6177 the analysis and modeling of the Adriatic Magnetic Anomaly (AMA, Figure 1b-d). The AMA represents the
62
63
64
65

78 most prominent geophysical feature within the Adria plate due to the paucity of seismicity with respect to
1
279 the neighboring chains (Faccenna et al., 2014; Sun et al., 2019) and its moderate average crustal thickness
3
4
80 (~30 km – Nicolich, 2001; Šumanovac, 2010; Tassis et al., 2013). The first evidence of a ~100 km-wide and
5
6
81 ~400 km-long AMA was provided by the aeromagnetic map of Italy (AGIP, 1983; Chiappini et al., 2000;
8
9
82 Caratori Tontini et al., 2004). Later, the dataset was extended towards the Croatian mainland by Giori et al.
10
11
83 (2007) producing a larger coverage but still incomplete map over the AMA that was used to support a
12
13
84 regional-scale source rather than local smaller sources (Mancinelli et al., 2015). These findings, despite
15
16
85 based on incomplete data coverage, were later validated by inverse modeling over a full-coverage map
17
18
86 (Milano and Fedi, 2017).

21
2287 At full data coverage, the AMA extends over 200 km in the SW-NE direction and 400 km in the NW-SE
23
2488 direction along the Adriatic Sea with maximum anomaly values of ~370 nT (Figure 1c). When observed at
25
26
89 regularly-spaced color intervals the AMA shows two main peaks centered at UTM33N WGS84 coordinates
27
28
290 486000 E, 4873000 N and 557000 E, 4812000 N (Figure 1c) and a straight NW-SE boundary along the
30
31
91 Croatian onshore-offshore transition with a negative anomaly area also trending NW-SE in mainland
32
33
92 Croatia and Bosnia-Herzegovina. Conversely, the southwestern boundary is arcuate with a trend ranging N-
34
35
93 S to W-E from north to south of the boundary. In the southwestern Central Adriatic the magnetic anomaly
37
38
94 is alternatively mapped by positive and negative spots while more towards the west and southwest, on the
39
40
4195 Italian shoreline and onshore areas, three main highs (A, B and C) are found (Figure 1c). Anomaly A (~85 nT)
42
43
96 is centered at 395000 E, 4825000 N few km offshore the Ancona promontory; anomaly B (~130 nT) is
44
45
97 centered at 442000 E, 4681000 N and anomaly C (~170 nT) is centered at 483000 E, 4617000 N on the
46
47
98 Abruzzo-Molise onshore. These three highs in the Apenninic foreland domain are relatively closer to the
49
50
99 AMA from south to north with decreasing distances along the SW-NE direction from 200 to 100 km.

51
52
53
100 The AMA shows clear and sharp northern and eastern boundaries while the western and southern
54
55
101 boundaries are less obvious and possibly blurred with surrounding anomalies. When compared with the
56
57
102 Bouguer gravity anomaly map of the area (Figure 1d), the AMA northeastern boundary clearly relates to the
59
60
103 boundary of the NW-SE Bouguer gravity minimum mapped over the Dinarides, while all the other AMA
61
62
63
64
65

104 boundaries do not match with gravity highs or lows. The AMA locates the only clearly observable magnetic
1
105 signal at satellite altitude over Southern Europe (Milano et al., 2019) and thus it certainly represents a deep
3
106 and regional-scale feature that is related to the geodynamic evolution of the Adria plate and whose source
5
6
107 cannot be limited to the outcropping gabbroic intrusions. To date however, the geodynamic context that
8
9
108 led to the emplacement of the causative source of the AMA was never investigated. Similarly, eventual
10
11
109 relations between the AMA and the A-C surrounding positive anomalies were never investigated despite
12
13
110 some authors (Minelli et al., 2018; Mancinelli et al., 2019) suggested that the B anomaly is related to high
15
16
111 magnetic susceptibility (~ 0.05 SI units) sources at the base of the crust.
17

112

20
21
22
23
24
25
26
27
28
29
30
31
32
33
34
35
36
37
38
39
40
41
42
43
44
45
46
47
48
49
50
51
52
53
54
55
56
57
58
59
60
61
62
63
64
65

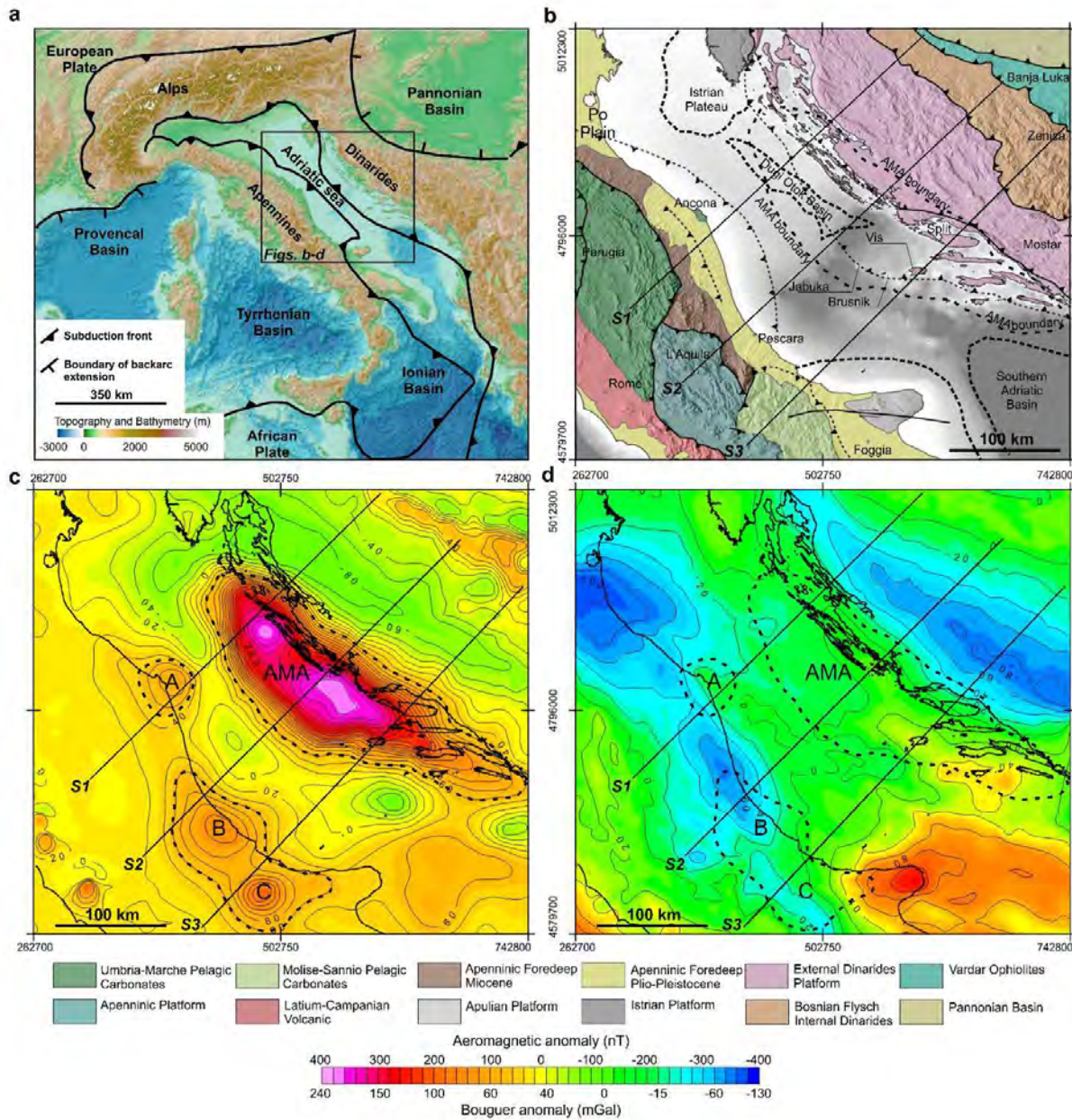


Figure 1 Geodynamic, geological and geophysical characters of the Central Adriatic Sea and surroundings. **a**, Actual geodynamic settings of the Central Mediterranean Sea and location of the study area. **b**, Simplified geological sketch map over the Central Adriatic Sea, Apennines and Dinarides (CNR – PFG, 1991; van Unen et al., 2019). **c**, Aeromagnetic total field anomaly at 2500 m height showing the AMA and A-C positive anomalies after Caratori Tontini et al. (2004) and Milano and Fedi (2017). **d**, Bouguer gravity anomaly over the modeled area (reduction density of 2670 kg m⁻³) after Tassis et al. (2013) and data over Italy and surroundings (CNR – PFG, 1991). Black continuous lines in b-d locate the modeled sections (S1-S3). Coordinates in this and following figures are in UTM33N WGS84.

Data and Methods

124 Available deep seismic data across the area are limited to the CROsta Profonda (CROP) profiles (Scrocca et
1
125 al., 2003) that across the Adriatic Sea generally show poor data quality below 7 s two-way-time (TWT) with
3
126 an exception given by CROP M17C crossing the area NNW-SSE (Figure 2 and S1). To our knowledge, crustal-
5
6
127 scale seismic data are lacking across external and internal Dinarides. Several other commercial seismic
8
128 profiles were acquired for hydrocarbon prospection but these were always limited in depth to 6 or 7 s TWT.
10
129 Similarly, tens of boreholes were drilled in the Central Adriatic Sea for exploration purposes but these never
12
130 reached the pre-Permian deposits across the entire Central Adriatic Sea (Scisciani and Esestime, 2017).
15

131 To address the open questions about the AMA and provide a plausible geodynamic interpretation of the
18
132 causative source, we created forward models of the observed aeromagnetic anomaly and Bouguer gravity
20
133 along three SW-NE trending ~400 km-long sections extending from the onshore Central Italy through the
23
134 Adriatic Sea, onshore Croatia and Bosnia-Herzegovina (S1-S3 in Figures 1 and 2).
25

135 A fundamental constraint when modeling magnetic anomalies is given by the Curie isotherm. Here, we set
28
136 a magnetite Curie temperature of 600 °C (Frost and Shive, 1986; Shive et al., 1992). To locate the Curie
30
137 isotherm we assume an average crustal thermal conductivity of 2.5 W m⁻¹ K⁻¹ (Turcotte and Schubert, 2002;
33
138 Pauselli et al., 2006; Pauselli and Ranalli, 2017) and calculate the conductive thermal gradient using heat
35
139 flow data from Central Italy (Pauselli et al., 2019), the Adriatic Sea (Della Vedova et al., 2001) and heat flow
38
140 values from Bosnia-Herzegovina (Atlas of geothermal resources in Europe, 2002). We also use thermal
40
141 gradient data over Croatia (Kurevija et al., 2014).
42

142 The observed conductive heat flow (q) is given by:

$$q = -k \frac{\partial T}{\partial Z}$$

143
144 where k is the thermal conductivity of crustal rocks and $\partial T/\partial Z$ is the thermal gradient (Fourier, 1822).
52

145 The resulting Curie depth is estimated to range between 35-40 km in the Apenninic and Adriatic areas,
56
146 where lower heat flow values (30-40 mW m⁻²) are observed, and ~20 km in the northeastern part of the
58
147 investigated area of Bosnia-Herzegovina, where the highest thermal gradient (30 K km⁻¹) and heat flow
60

148 values ($\sim 75 \text{ mW m}^{-2}$) are found. Considering that the Moho discontinuity represents a magnetic boundary
 1
 149 preventing any contribution from the mantle to generate anomalies (Wasilewski et al., 1979; Wasilewski
 3
 150 and Mayhew, 1992), these estimates allow to assume that the observed magnetic anomalies may come
 4
 5
 6
 151 from sources located within the entire crust in the Apenninic, Adriatic and Croatian onshore domains, while
 8
 9
 152 sources in the northeastern area are located within the upper crust.

10
 11
 12
 153 We set the parameters of the magnetic field according to the geomagnetic epoch 1979 (Caratori Tontini et
 13
 14
 154 al., 2004) of the L'Aquila geomagnetic observatory (<https://roma2.rm.ingv.it/>): field intensity (H) 36.8 A/m,
 15
 16
 155 inclination (I) 58°, declination (D) -0.1°. In modeling the magnetic anomalies we consider both induced
 18
 19
 156 (M_i) and remanent magnetization (M_r). The first is attributed through the magnetic susceptibility ($M_i = S \times H$)
 20
 21
 157 to each body above the Curie depth. The remanent magnetization is attributed through field inclination of
 22
 23
 158 0° and declination of 12° (Table 1), only to modeled volumes above the 400°C isotherm because at higher
 25
 26
 159 temperatures M_r contributions are unlikely due to its unstable and viscous signature (Pullaiah et al., 1975;
 27
 28
 160 Schlinger, 1985; Minelli et al., 2018). In our modeling, we set a maximum magnetic susceptibility of 0.05
 30
 31
 161 ± 0.005 (SI units) compatible with estimates of Minelli et al. (2018) and modeling in the Central Apennines
 32
 33
 162 by Mancinelli et al. (2019). All other bodies modeled across the sections were given susceptibility values
 34
 35
 163 ranging between 0 and 0.055 SI units. Table 1 shows the magnetization parameters used for the modeled
 37
 38
 164 bodies.

165

	Remanent magnetization (A m^{-1})	Magnetic susceptibility (SI units)
Permian-to-recent sedimentary units	0	0
Paleozoic basement	0	0.001
Paleozoic basement with Gabbroic intrusions	5	0.055
Underplated volume	1.5	0.055

166 **Table 1. Magnetic susceptibility and remanent magnetization of the modeled bodies.** The remanent
 167 magnetization is modeled with field inclination of 0° and declination of 12° according to the Permian
 168 paleopole (Van der Voo, 1990). Values of remanent magnetization and magnetic susceptibility are taken
 169 from literature (Rochette, 1994; Bronner et al., 2011; Minelli et al., 2018).

170

58
 59
 60
 61
 62
 63
 64
 65

171 The high magnetic susceptibilities used to model the main source of the AMA and surrounding magnetic
1
172 anomalies exclude the possibility of a granitic composition for these bodies (Punturo et al., 2017) but
3
173 suggest a serpentinitic composition of the underplated volume (Rochette, 1994). Bearing in mind the non-
5
6
174 uniqueness of the geophysical forward modeling, in the following section we present the models resulting
8
9
175 from the combined interpretation of gravity and magnetic anomalies along the three profiles.

176 177 **Results**

178 The modeled sources extend upwards from the Moho discontinuity through the crust with higher density
17
179 and magnetic susceptibility (≥ 0.05 SI units) than the surrounding volumes. The modeled susceptibility
19
20
180 values related to deep sources are comparable to those found in the Central Apennines (Minelli et al.,
22
23
181 2018; Mancinelli et al., 2019). Minimum thicknesses of the sources are observed toward model ends, both
24
25
182 NE and SW, and beneath the Central Adriatic Sea. However, lateral continuity is never interrupted along all
26
27
183 the three models. The shape of the magnetic sources results coherently from the modeled sections in the
29
30
184 form of an asymmetric crustal batholith whose basal layer widens southwards (Figure 2a-c). The thickness
31
32
185 of the source increases northeastwards to maximum values of ~ 20 km along sections S1 and S2 beneath the
34
35
186 Croatian archipelago, while its lateral extent ranges between 250 and 400 km from north to south. Beneath
36
37
187 the Dinaric belt, the modeled AMA source base is at ~ 20 km depth due to shallower Curie isotherm, but we
38
39
188 can speculate that also the volumes constituting the crustal root of the Dinarides may have undergone the
41
42
189 same processes because the modeled density values fit the AMA source density. The AMA source is
43
44
190 laterally asymmetric also considering its upper bound because in the Dinaric domain the top of the source
45
46
191 propagates to depths significantly shallower than in the Adriatic domain (Figure 2). Given the evidence of
48
49
192 significant volume transfer from Adria to the Dinarides during their Eocene-to-present collision (Bennett et
50
51
193 al., 2008; Le Breton et al., 2017; Handy et al., 2019), we speculate that this asymmetry is representative of
53
54
194 tectonic reworking of the AMA source during the Adria-Eurasia collision.

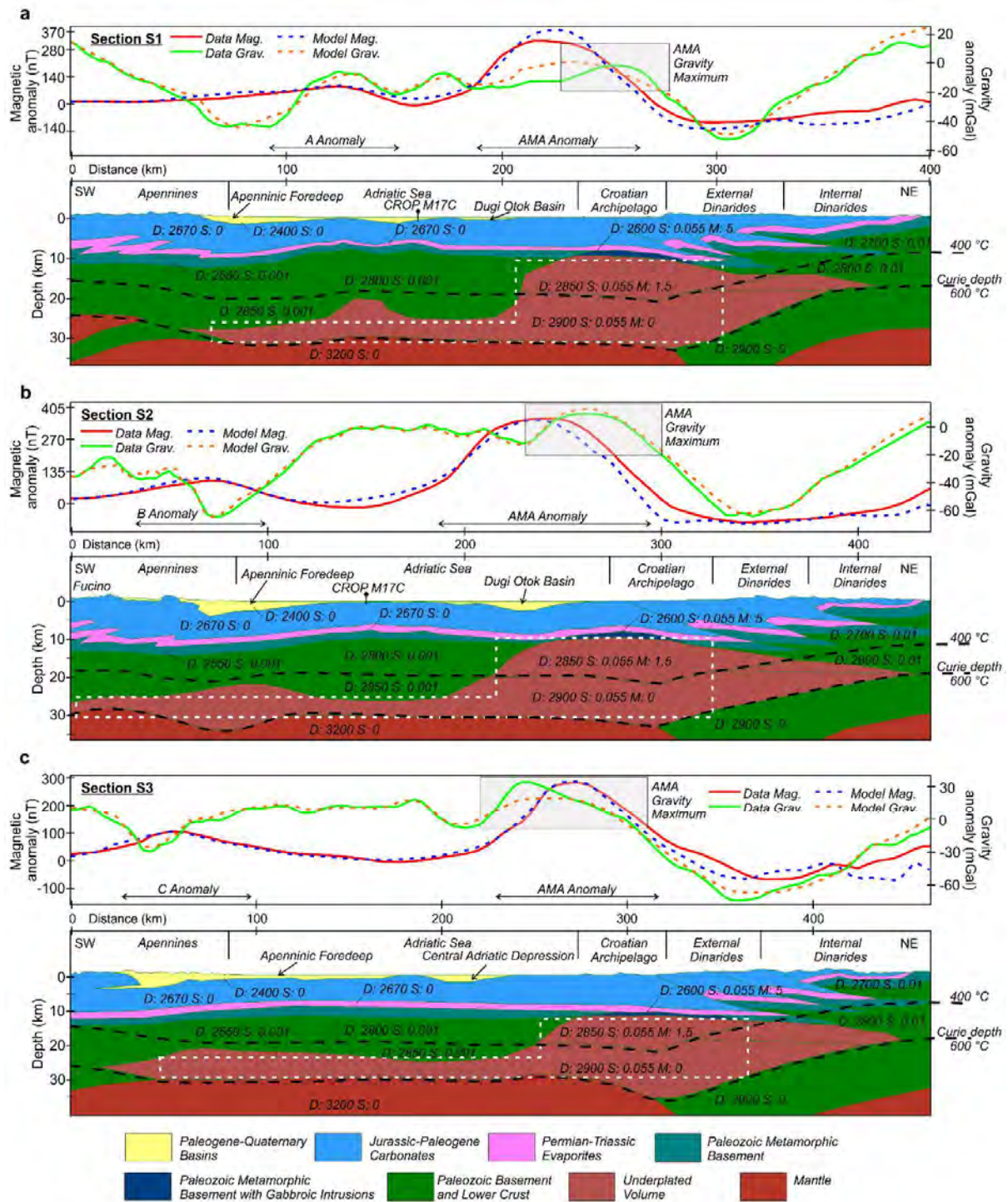


Figure 2. Forward modeling of the S1-S3 sections. a, Magnetic and gravity anomalies forward modeling across section S1. **b,** Magnetic and gravity anomalies forward modeling across section S2. **c,** Magnetic and gravity anomalies forward modeling across section S3. Modeled density (D) and magnetic susceptibility (S) values are indicated for each body. Remanent magnetization (M) is assigned only to high susceptibility volumes above the 400 °C isotherm. Areas bounded by white dashed lines locate the volumes considered for estimation of the volume of the magnetic sources. Vertical-to-horizontal scale ratio across the modeled sections is 0.5. Reference starting values for the Moho depth across the modeled area are from literature (Scarascia et al., 1998; Šumanovac, 2010; Tassis et al., 2013). Similarly, the starting density values of the

205 modeled bodies and geometries of the sedimentary units are retrieved from literature (Fantoni and
206 Franciosi, 2010; Mancinelli et al., 2015; Montone and Mariucci, 2015; Scisciani and Esetime, 2017; van
207 Unen et al., 2019; Montone and Mariucci, 2020; Mancinelli and Scisciani, 2020; Mancinelli et al., 2021; and
208 references therein).

209

6

7

210

9

211

11

212

12

213

14

214

18

215

19

216

21

217

23

24

218

27

219

28

220

29

221

30

222

31

223

32

224

33

225

34

226

35

227

36

228

37

229

38

230

39

231

40

232

41

233

42

234

43

235

44

236

45

In the upper crust, the AMA source reaches a minimum depth of ~9 km NE of the Dugi Otok depression along section 2 (Figure 2b) propagating with gabbroic intrusions through the upper basement. This suggests that the Triassic evaporites postdated the AMA source, whose emplacement probably ended in Early or Middle Permian. Thus, our modeling supports the latter dating of the gabbroic intrusions on Jabuka and Brusnik islets (Palinkaš et al., 2010) rather than previous estimates proposing younger ages. The gabbroic intrusions in the basement were later locally exhumed by compressional and transpressional tectonics (Tari, 2002) related to the Dinaric chain emplacement and are those outcropping in the Croatian archipelago.

The observed magnetic anomalies over the Central Adriatic Sea and surroundings are thus prevalently related to deep sources with small contributions from low susceptibility lower crust and basement. Given the spatial distribution at the base of the crust and the magnetization of the modeled bodies, these sources are interpreted as thin gabbroic intrusives overlying a massive underplating beneath the Adria s.str. microplate. While the shallowest expression of the magnetic source is given by the intruded gabbros in the upper basement, the nature of the underplated volume is constrained by the high susceptibility values required to model its sources, suggesting a lower crust enriched in serpentine (Rochette, 1994). This view is also supported by the Bouguer gravity anomaly because local maximums of the observed gravity are found over the AMA in all the modeled sections (Figure 2a-c) suggesting that the cooling of the underplated and intruded material has increased also the density of the lower crust. If our interpretation is correct, the modeling provides an estimate of the longitudinal extent of the underplated material that may range up to ~400 km. Furthermore, the modeled sections suggest that given its volume and extent, the underplated material represents an episode of massive and large-scale magmatic activity of Permian age rather than Triassic (Cassinis et al., 2012).

232 To estimate the volume of the causative source for the observed magnetic anomalies we use the minimum
1
233 values of thickness and lateral extent (SW-NE direction) of the source as resulting from the modeled
3
234 sections (white dashed polygons in **figure 2**). Furthermore, we consider the distance between section 1 and
4
5
6
235 3 (~180 km) to represent the third dimension of the source along the NW-SE direction. Only volumes with
8
236 strong induced and/or remanent magnetization are considered (magnetic susceptibility ≥ 0.05 SI and/or
10
11
237 remanent magnetization $\geq 1.5 \text{ A m}^{-1}$). From this estimate we exclude the volumes outside the white dashed
12
13
238 boxes in **figure 2** – i.e. the northernmost wedge-shaped anomalous sources and the A-C sources, due to
15
16
239 their marked lateral variability. This approach provides a conservative estimate of the AMA source volume
17
18
240 ($0.3 \times 10^6 \text{ km}^3$) and of the underplated material beneath the Adriatic Sea and Italian onshore ($0.2 \times 10^6 \text{ km}^3$).
20
241 Thus, the modeled high-susceptibility sources total volume is $\sim 0.5 \times 10^6 \text{ km}^3$, encompassing both the
22
242 underplated and intruded material and accounting also for the small portions of the upper crustal volumes
24
25
243 hosting the shallow gabbroic intrusions.
26
27
28
244

245 Discussion

33
34

246 Considering the volumes of the underplating and of the intruded gabbros as resulting from the modeling
36
247 and their transparency as shown in deep seismic profiles imaging in the area (**figure S1**), we can speculate
38
39
248 that after the underplated and intruded material was supplied, it has undergone a long-lasting cooling and
41
249 solidification period (Thybo and Artemieva, 2013). This implies that in the Adria s.str. area the continental
43
44
250 breakup never evolved to oceanic spreading with new crust formation but it aborted soon after the first
45
46
251 underplating phase, following an evolution similar to that proposed for the Permian igneous and
48
49
252 metamorphic rocks in the European Alps by Schuster and Stüwe (2008). This supposed interruption of the
50
51
253 breakup evolution is supported by the lack of volcanic evidence from outcrops and boreholes in the entire
52
53
254 Central Adriatic Sea because short timings ($< 0.1 \text{ Ma}$) are required between underplating and the following
55
56
255 magmatism (Petford et al., 2000; Thybo and Artemieva, 2013). However, we suggest that some
57
58
256 consequences of the aborted rift in the Central Adriatic Sea are still evident.
59
60
61
62
63
64
65

257 In **figure 3** we compare the top of the underplated and intruded volumes against the distribution of known
1
258 long-lasting carbonate platforms and Permo-Triassic structural highs in the Central Adriatic and
2
3
259 surroundings. These regions locate palaeogeographical scenarios that never evolved to slope or basin
4
5
6
260 domains during Jurassic or Cretaceous times (Dinaric platform) or made their transition during Triassic or
7
8
261 Jurassic, with significant delay when compared to surrounding depositional sequences. Among the latter,
9
10
11
262 we include the Ancona and Villadegna highs where stratigraphic evidence (Cazzola and Soudet, 1993;
12
13
263 Scisciani and Esetime, 2017) suggest that palaeogeographical domains during Triassic and Early Jurassic
14
15
264 were tectonically controlled. In these areas, the uplifted regions resulted in longer-living shallow water
16
17
18
265 environments while these were surrounded by deeper conditions such as the Emma and the East Gran
19
20
266 Sasso basins located east and west of the Villadegna area, respectively (Scisciani and Esetime, 2017). In the
21
22
267 case of anomaly C such evidence is buried beneath ~12 km of overlying Apulian platform and Southern
23
24
268 Apennines foredeep deposits (Butler et al., 2004) that cover the westward-subducting Adria crust and
25
26
269 prevents any detection of eventual Permian uplift related with Adria crustal evolution.
27
28
29
30
31
32
33
34
35
36
37
38
39
40
41
42
43
44
45
46
47
48
49
50
51
52
53
54
55
56
57
58
59
60
61
62
63
64
65

1
2
3
4
5
6
7
8
9
10
11
12
13
14
15
16
17
18
19
20
21
22
23
24
25
26
27
28
29
30
31
32
33
34
35
36
37
38
39
40
41
42
43
44
45
46
47
48
49
50
51
52
53
54
55
56
57
58
59
60
61
62
63
64
65

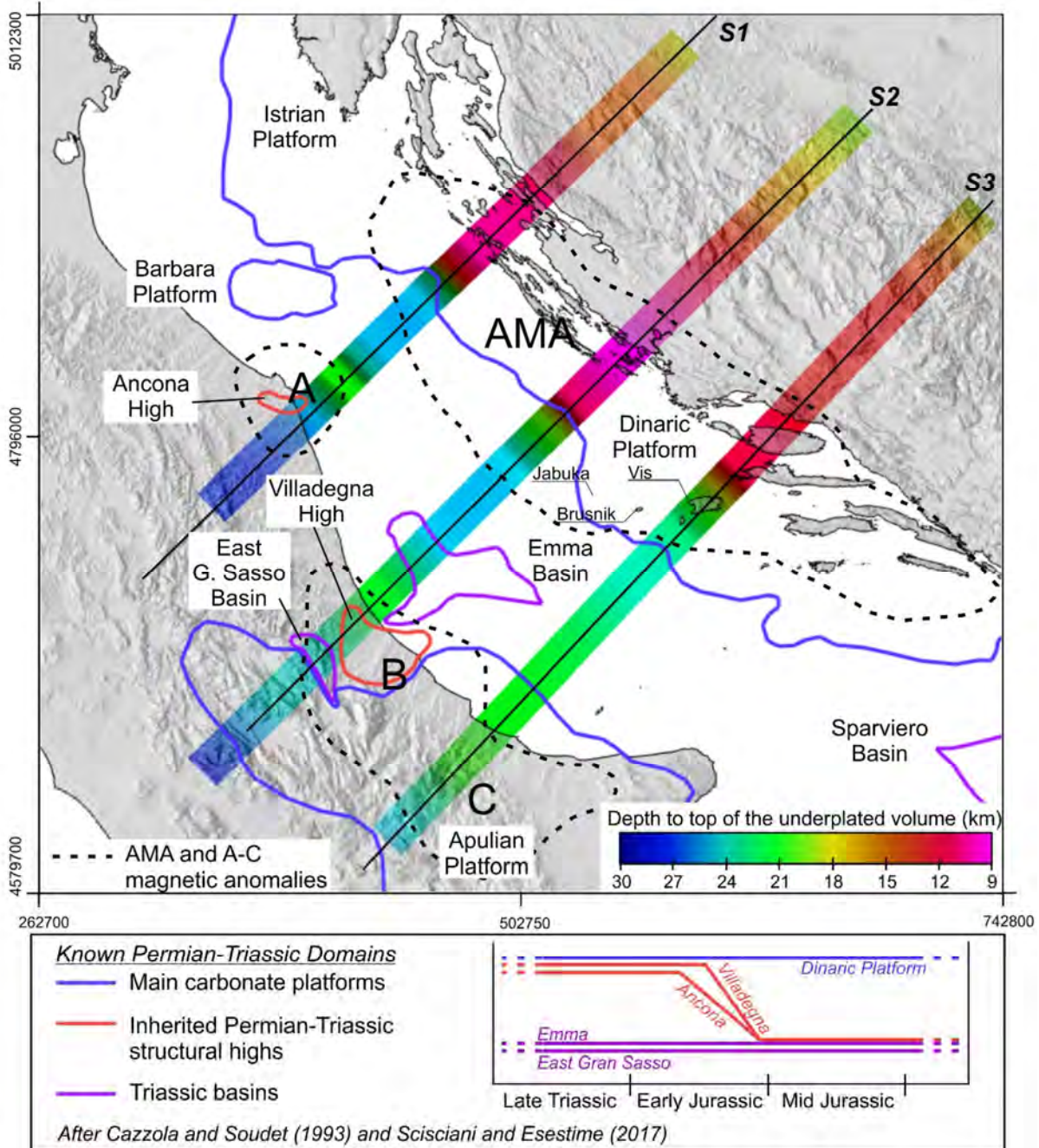


Figure 3. Comparison between the modeled underplated and intruded volumes and known Adria Permian-Triassic domains. The spatial trend of the top of the underplated and intruded volumes (color-coded bands) is compared against the boundaries of the mapped magnetic anomalies (dashed black lines) and the spatial distribution of the known palaeogeographical domains in Late Permian-Early Triassic (color-coded lines). The drowning timing of the inherited structural highs is also provided in the lower plot and compared to surrounding basins and the Dinaric platform. The north-eastern areas where shallower magnetic sources are found along modeled sections S1 and S2, match the boundary of the long-living Dinaric carbonate platform. The south-western areas below the A-C anomalies correspond to inherited structural highs from Permian uplifted regions (A and B) and to a region of Adriatic affinity beneath the Apulian platform and Southern Apennines foredeep (C). The current position of the East Gran Sasso basin

281 results after ~10 km of eastward-directed shortening related to the Apenninic orogenesis (Viandante et al.,
282 2006).

2
283

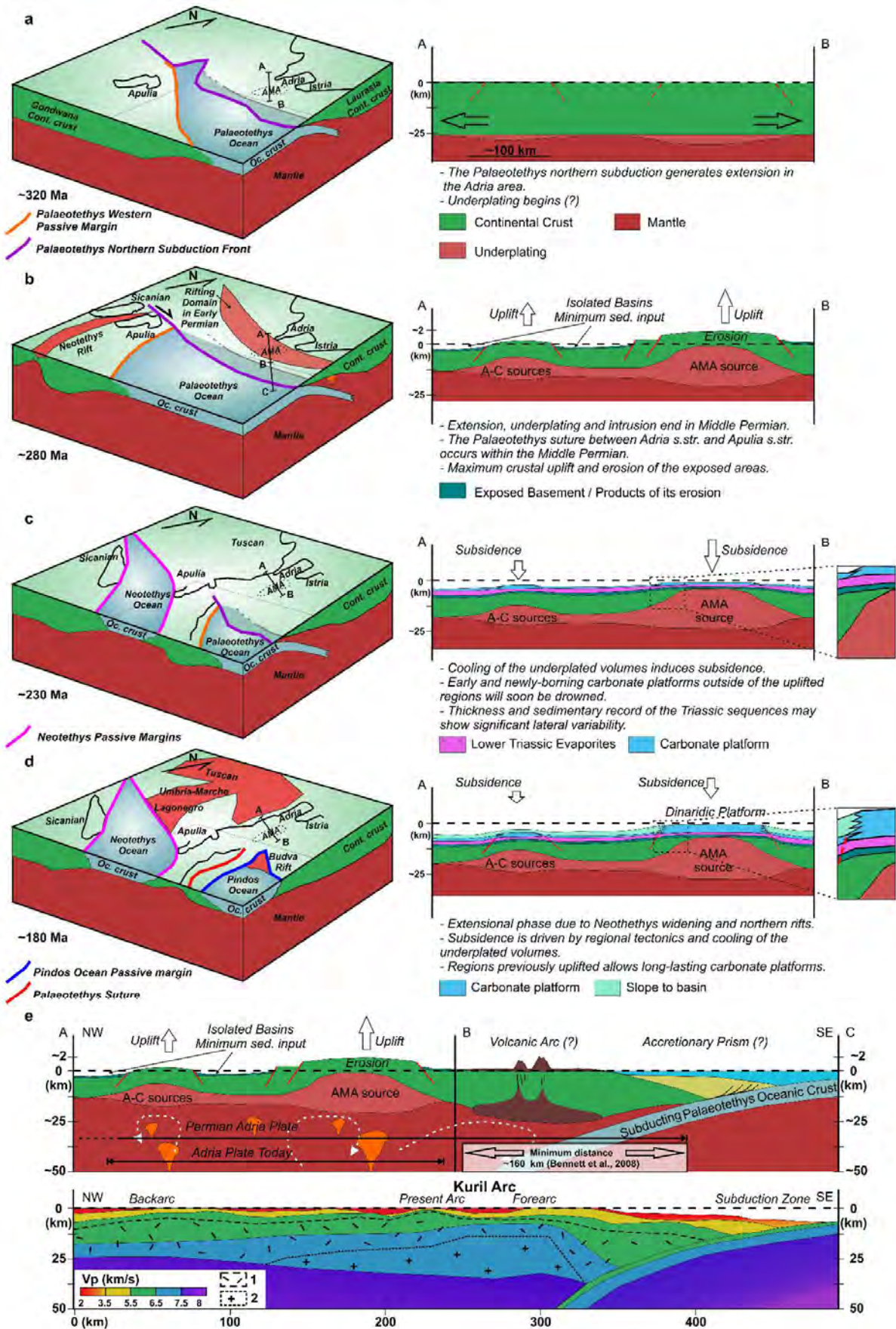
4
5
284 The fitting between the modeled deep crustal magnetic source and these regions is surprising and
6
7
285 intriguing. Considering the spatial distribution of such domains and the marked asymmetry across the
8
9
286 Central Adriatic given by the thick and continuous Dinaric platform (Scisciani and Esestime, 2017) compared
10
11
287 to the scattered structural highs and basins in the Western Adriatic area, we speculate that the causes for
12
13
288 such evidence are related to regional-scale phenomena affecting the tectonic setting of the upper crust.
14
15

16
17
289 Furthermore, we suggest that the observed heterogeneity in the palaeogeographical Permian and Triassic
18
19
290 domains is a direct consequence of the underplated and intruded material that over-compensated the rift-
20
21
291 related crustal thinning resulting in uplifted regions of crust corresponding to major underplated volumes
22
23
292 (figure 4a-b).

24
25
26
27
293 The basement that was exhumed because of the underplating was partially eroded during Permian allowing
28
29
294 the intruded gabbros to further shallow. After an evaporitic sedimentation phase in Early Triassic, whose
30
31
295 products show heterogeneous thickness and distribution across the area (figure 4c; Scisciani and Esestime,
32
33
296 2017), carbonate platforms lasted longer in the uplifted regions and were preserved since Cretaceous with
34
35
297 respect to the surrounding regions where marginal and basin conditions developed since Triassic times
36
37
298 (figure 4c-d). Such a heterogeneous scenario implies that the flexural strength of the crust was very low or
38
39
40
299 null, a view that is compatible with the continental breakup phase and the related crustal thermal regime
41
42
300 (Scivetti et al., 2021) and with widespread transcurrent and extensional deformation in western Europe in
43
44
301 Permian times (e.g. Molli et al., 2020).

45
46
47
48
49
302 We propose that the underplating is related to back-arc extension in the frame of the Palaeotethys-Adria
50
51
303 s.str. convergence (Figure 4e). Such an event could have been driven by dehydration of the subducting
52
53
304 Palaeotethys oceanic crust beneath Adria s.str. The resulting hydrous mantle gathered at the base of the
54
55
305 crust and infiltrated through it causing uplift, thinning and heavy serpentinization of the crust that, by the
56
57
58
306 end of Early Permian, was resembling a magma-poor ocean-continent transition. Scenarios involving back-
59
60
307 arc extension were common in the northern Palaeotethys margin (Stampfli et al., 2004) due to the
61
62
63
64
65

308 acceleration of Palaeotethys slab rollback after the end of Gondwana and Laurasia convergence and
1
309 collapse of the Lurasian active margin (Vavassis et al., 2000). The back-arc regions firstly evolved towards
3
310 shallowing or exhumation of the lower crust over large areas in a Basin and Range fashion (Zandt et al.,
4
5
6
311 1995), and finally towards opening of the small Triassic back-arc oceans (Meliata, Maliak, Pindos-Huglu)
8
312 (Stampfli and Kozur, 2006). The thickness and nature of the magnetic source as retrieved from our
10
11
313 modeling and the trace element composition of the gabbros outcropping in the Croatian archipelago
12
13
314 (Figure 5) argue against other possible origins of the underplating.
15
16
315
18
19
20
21
22
23
24
25
26
27
28
29
30
31
32
33
34
35
36
37
38
39
40
41
42
43
44
45
46
47
48
49
50
51
52
53
54
55
56
57
58
59
60
61
62
63
64
65



1
2
3
4
5
6
7
8
9
10
11
12
13
14
15
16
17
18
19
20
21
22
23
24
25
26
27
28
29
30
31
32
33
34
35
36
37
38
39
40
41
42
43
44
45
46
47
48
49
50
51
52
53
54
55
56
57
58
59
60
61
62
63
64
65

Figure 4 Conceptual models of the formation and Permian-Jurassic evolution of the underplated volume.

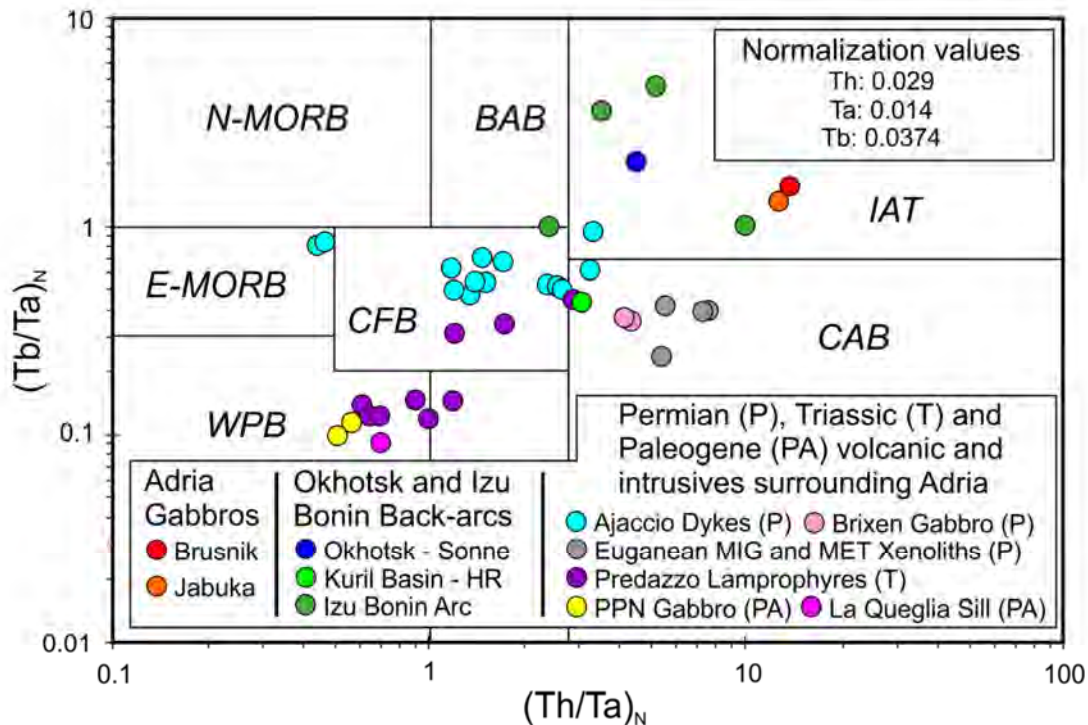
a, Late Carboniferous palinspastic sketch illustrating the Adria s.str. and Apulia s.str. microplates and surroundings; due to the inception of back-arc spreading the underplating possibly started during the widening of the Palaeotethys Ocean. **b**, During Early Permian the increasing underplated volume provides substantial uplift in the areas where the major volumes are localized. In Middle Permian, the opening of the Neotethys western branch stops the underplating and prevents breakup completion. Sedimentation in internal basins is limited and localized, mostly consisting of erosional products of the exposed basement. **c**, In a period of tectonic stasis due to the closing of the northern Palaeotethys branch, post-underplating subsidence has produced its effects and Triassic evaporites are deposited above the basement. **d**, During Late Triassic and Lower Jurassic the regions that undergone higher uplifts in the previous period allow the Dinaric carbonate platform to grow longer, while in adjacent areas slope and deeper environments are found. The opening of the Umbria-Marche and Lagonegro basins is lateral (westwards) to the Adria s.str. microplate but likely contributes to tectonic subsidence of the western Adria basins. **e**, Regional model section across the subducting Palaeotethys oceanic crust and the study area during Early Permian (for location see **figure 4b**) compared with the P-wave velocity model across the Kuril arc (Nakanishi et al., 2009) and its interpretation after Thybo and Artemieva (2013) – 1: Post-fractionation and delaminated underplating; 2: Mafic underplating. Orange polygons and white dashed lines in **figure 4e** denote serpentinized diapirs and mantle circulation, respectively. Palaeogeographic maps are modified after Moix et al. (2008), Stampfli and Hochard (2009), Stampfli et al. (2013).

Geometries of the modeled volumes may suggest a tectonic underplating process (Menant et al., 2019) related to the Palaeotethys subduction beneath Adria in the Early Permian. In this scenario, the outcropping gabbros and the underplated volume would represent the lower Palaeotethys oceanic crust tectonically stacked during its subduction beneath Adria. Though the observed topographic uplift seems to support this view (Menant et al., 2020), a tectonic origin for the underplating can be ruled out because of the timing, thickness and nature of the underplated material. In fact, the ~20 km thick underplated volumes are significantly younger than the Palaeotethys oceanic crust. Furthermore, the thin and deep gabbroic oceanic crust is not involved by tectonic stacking that should allow underplating only of the upper basaltic layers (Menant et al., 2019) that are missing across the entire study area.

An alternative view could regard the AMA source as a fossil seamount pertaining to the Palaeotethys ocean that was exposed by erosion of the accretionary prism once the Palaeotethys was closed. The size of the AMA source is compatible with other cases along the Palaeotethys suture (Moix et al., 2008; Federici et al., 2010; Moix et al., 2013; Eyuboglu et al., 2018) but the basaltic, ophiolitic and metamorphic facies that usually are found in such cases are missing in the Central Adriatic area. Moreover, a seamount origin for the

351 outcropping gabbros is further discredited by their trace element concentration that supports an Island-Arc
 1
 352 origin (Figure 5).

353 Another plausible alternative scenario can relate the AMA underplating to the northwestern termination of
 6
 354 the Pindos ocean – i.e. the Budva rift (Stampfli and Kozur, 2006; Moix et al., 2008). Given the Budva-Adria
 9
 355 proximity in Late Triassic-Early Jurassic times (figure 4), if the Budva rift survived to the Pindos subduction,
 11
 356 its attenuated lithosphere may have carried the AMA underplating and the intruded gabbros towards the
 13
 357 external Dinarides during later transcurrent deformation (Stampfli and Kozur, 2006). In such case however,
 16
 358 the AMA and its causative source should be located at least in the external Dinarides or, given the Cenozoic
 18
 359 Adria-Eurasia collision, it should be even more internal on the Dinaric chain. Furthermore, this hypothesis is
 20
 360 not matched by the Triassic evaporites postdating the intruded gabbros as resulting from our modeling
 23
 361 (figure 2).



363
 364 **Figure 5. $(Th/Ta)_N$ vs $(Tb/Ta)_N$ ratios (Thièblemont et al., 1994) for the gabbros outcropping in Jabuka**
 365 **and Brusnik islands compared with surrounding known Permian-Triassic volcanics and intrusives and**
 366 **with the Okhotsk-Kuril back-arc and the Izu Bonin back-arc volcanics. N-MORB field – N-Type MORB;**
 367 **E-MORB field – E-Type MORB; BAB field – Oceanic back-arc basin basalt; WPB field – Within-plate**
 368 **basalt (transitional and alkaline); CFB field – Continental tholeiite; IAT – Island-arc tholeiite; CAB –**

369 Subduction-related calc-alkaline lava. These data exclude a basaltic composition and a seamount origin
370 for the gabbros outcropping in Jabuka and Brusnik (see **Figure 1** for their locations). Brusnik and Jabuka
371 compositional data are from Radić and Lugović (2004). Data from the Sonne central volcano in the
372 Okhotsk Sea and from the Hydrographer Ridge (HR) in the Kuril Basin correspond to samples 126-1-1,
373 126-1-2, DR7-1-1, DR7-1-2 and DR83-1-1 from Werner et al. (2020). Data from the Izu Bonin arc are
374 from Straub (2003). Data from the Ajaccio dykes and Brixen gabbros are from Boscaini et al. (2020).
375 Data for the Migmatite (MI) and Metapelite (ME) xenoliths from the Euganeans hills are from Sassi et
376 al. (2020). Data from the Predazzo lamprophyre are from Casetta et al. (2019). Data from the Punta
377 delle Pietre Nere (PPN) gabbros are from Mazzeo et al. (2018). Data from the La Queglia sill on the Gran
378 Sasso range are from Avanzinelli et al. (2012). All data are normalized against CI Chondrites (Sun and
379 McDonough, 1989).

380
381 **Figure 5** shows that when compared against data from an actual island-arc system in the Okhotsk Sea and
382 Kuril Basin (Werner et al., 2020), the trace element composition of the Jabuka and Brusnik gabbros suggests
383 that these are related to an internal back-arc area of the island-arc system. In fact, Jabuka and Brusnik
384 samples show a better fit with the Sonne samples (~300 km from the Kuril arc) rather than with the
385 Hydrographer Ridge (HR) samples (~80 km from the Kuril arc). Moreover, the Jabuka and Brusnik samples
386 are comparable also with the Izu Bonin back-arc volcanics (Straub, 2003). The trace element composition of
387 the gabbros from Jabuka and Brusnik do not compare with the composition of the surrounding known
388 Permian-Triassic volcanics and intrusives where such data are available. In fact, age and composition of the
389 Jabuka and Brusnik gabbros do not compare with the Punta delle Pietre Nere gabbroic outcrops in the
390 Gargano promontory. These latter bodies, are significantly younger (58- 62 Ma) than those in the Croatian
391 archipelago, were tectonically emplaced in Plio-Pleistocene times (Mazzeo et al., 2018 and references
392 therein) and were possibly remagnetized during a reverse recent period (Speranza and Kissel, 1993). Finally,
393 age and composition of the Jabuka and Brusnik gabbros do not compare either with data from the
394 Eocene(?) La Queglia sill on the Gran Sasso range (e.g. Satolli et al., 2005; Avanzinelli et al., 2012).

395 In **figure 4e** we show an interpretative view of the Palaeotethys-Adria s.str. boundary in Early Permian
396 suggesting that this convergent margin was similar to the actual Pacific-Okhotsk plate boundary where
397 underplating contributes to crustal accretion beneath and behind the Kuril arc (Nakanishi et al., 2009;
398 Thybo and Artemieva, 2013). In this scenario, the minimum distance between the AMA anomaly and the
399 Palaeotethys subduction front was ~150 km (**figure 4e**). This spatial reference is compatible with the

400 proposed collisional scheme and with the regional palaeogeographic Permian scenario (Stampfli et al.,
1
401 2013). Moreover, this interpretation is further supported by the depth (~160 km) reached by the subducted
3
402 Adria slab beneath Dinarides during their Eocene-to-present collision (Bennett et al., 2008).
5
6

7
403 If the rifting was completed laterally (southwards) to the Adria s.str. microplate or if it evolved
8
9
404 discontinuously and completion of the breakup was aborted only in this region remains unclear. However,
11
12
405 in the first case any evidence would have been consumed by the Adria subduction beneath the Dinarides,
13
14
406 whilst in the second case this portion of the Adria s.str. microplate was very close to the formation of new
15
16
407 oceanic crust, as testified by intrusive bodies reaching shallow depths, but a rapid change in the
18
19
408 geodynamic context has stopped rift completion between Early and Middle Permian. We suggest that this
20
21
409 event is the opening of the westernmost Neotethys branch that sets the stage to close the gap between the
23
24
410 Apulia s.str. and Adria s.str. microplates to form the wider Adria as it is today (figures 4b-4c), accelerates
25
26
411 the closure of the Palaeotethys ocean and stops the extensional tectonics in the Adria s.str. area (Figure 4c-
27
28
412 d).

30
31
413 Assuming an Airy-type response within the crust (Watts, 2001) we can estimate the maximum uplift
33
414 induced by the underplating load:
35
36

$$u = v \frac{(\rho_m - \rho_x)}{(\rho_m - \rho_w)}$$

37
415 where u is the induced uplift, v is the thickness of the underplated body, ρ_m is the density of the mantle
39
40
416 (3200 kg m⁻³), ρ_x is the density of the underplated body (2900 kg m⁻³) and ρ_w is the density of water (1030
42
43
417 kg m⁻³) (Watts, 2001). Table 2 shows the estimated uplift due to underplated material thickness ranging
45
46
418 between 2 and 25 km. If a regional uplift is assumed to be ~700 m due to the basal layer of the source
47
48
419 averaging 5 km thickness in all the modeled sections, the maximum uplift beneath the AMA source ranges
50
51
420 between ~2700 and 2000 m for underplating thicknesses of 25 and 20 km, respectively. Above the sources
52
53
421 for the A-C anomalies in Western Adriatic Sea and onshore Italy, the maximum estimated uplift is ~700 m
54
55
422 because of the average underplating thickness of 10 km across all modeled sections (Figure 2).
56
57
423
58
59
60
61
424
62
63
64
65

v (km)	2	5	10	15	20	25
u (m)	276	691	1382	2074	2765	3456

Table 2. Airy-type crustal uplift u (m) compared to the thickness of the causative underplated material v (km).

The above calculations provide a maximum uplift value in the Dinaric domain of ~ 2000 m. This estimate is supported by the differential growth of the Dinaric platform in respect to the Adriatic domain. In the first case, above the thicker and wider AMA source, we find a wide and continuous Dinaric carbonate platform lasting from Triassic to Paleogene (Scisciani and Esestime, 2017). In the Adriatic domain, above the thinner sources that we interpret as causative of the A and B anomalies, we find scattered duration of the carbonate platforms and structural highs (Figure 3) whose spatial distribution coincides with locations of the A and B anomalies and causative sources. The drowning of these latter domains was likely driven by faster cooling of the thinner underplated material accelerating upper crustal subsidence (Schuster and Stüwe, 2008) with possible later contributions from the western Jurassic rifting systems (Figure 3d).

In this framework, strong magnetic sources are lacking at the base of the southernmost Apulian s.str. crust (Figure 1c; Caratori Tontini et al., 2004; Milano et al., 2019) because during Late Carboniferous and Early Permian times the Apulia s.str. microplate pertained to the Cimmerian terranes and was in between the Palaeotethys and the newly-opening Neotethys (Stampfli et al., 2013), away from the Adria underplating (Figure 4b). If the Apulian promontory was in the same position relative to the Adriatic Sea (Figure 1) and/or should testify this with magnetic signatures like those found in the Central Adriatic Sea (Figure 1) and/or with massive Permian magmatic intrusions like those observed in the Alps (Cassinis et al., 2012) or resulting from our models. Such evidence is lacking because only one thin level of volcanic deposits is found interlayered in shallow-water carbonates of Apulian affinity across the complete Permian sequence drilled by the Gargano 1 borehole (Scisciani and Esestime, 2017). On the contrary, the C anomaly is apparently related to the Apulian platform (Figure 3) but it is actually related to the Early Permian underplating beneath the Adria s.str. microplate and thus pertains to the westward-subducting Adria s.str. crust.

449 If the linkage between the AMA source and the sources of the A- C anomalies is accepted, then some
1
450 constraints are provided to the extent of the Adria s.str. microplate. In fact, the boundary between Adria
3
451 s.str. and Apulia s.str. should be located south of the C anomaly. In this area surrounding the Gargano
5
6
452 promontory the lithosphere thickens southwards (Calcagnile and Panza, 1981) and broad E-W transform
8
9
453 deformation was related to inherited discontinuities in the deep crust (Di Bucci et al., 2006). Furthermore, a
10
11
454 significant GPS velocity increase was observed between the areas north and south of the Gargano
12
13
455 promontory (Oldow et al., 2002) and recent findings suggest that the Adria plate as intended today
15
16
456 extending from the Alps to the Apulian promontory, is fragmented in two subplates rotating in opposite
17
18
457 directions and whose boundaries are located in the Gargano promontory area (Handy et al., 2019). We
19
20
458 interpret all these features as indicative of the boundary between the Adria s.str. and Apulia s.str. grossly
22
23
459 corresponding with the E-W transform zone, but whose eventual upper crustal evidence was masked by the
24
25
460 Cenozoic Apenninic orogenesis. In this view, this area locates the Palaeotethys suture between the two
27
461 microplates occurred no later than Middle Permian. This Paleozoic plate boundary is still affecting the
29
30
462 geodynamic evolution of the area.
31

32
33
463
34

35 36 464 **Conclusions** 37

38
39
465 The case of the Adria plate demonstrates that underplating processes in collisional dynamics may
41
466 contribute to continental crust accretion and, in the long term, to preserve crustal thickness. This is the
43
44
467 case in the Pacific-Okhotsk plate boundary as it was in the Palaeotethys-Adria s.str. collision. Underplating
45
46
468 contribution is showcased by the long-living Dinaric carbonate platform whose evolution since Permian
48
469 times would have been completely different without the underplated volume that, by providing significant
50
51
470 uplift and crustal buoyancy, has controlled the topography/bathymetry ultimately allowing for platform
52
53
471 growth and palaeogeographic differentiation. In the long-term evolution of the plate, the underplated
55
56
472 volume has probably played a key role also in the Adria-Eurasia collision by partial transfer of crustal
57
58
473 volumes from the Adria plate to the Dinaric belt.
59
60
61
62
63
64
65

474 **Acknowledgments and data availability**

1
475 The authors acknowledge the constructive and insightful comments of Giancarlo Molli and Ingo Heyde and
476 the editorial handling of Tiago Alves. All the data used in this work are available from literature and
477 published maps.
5

6
478 **Competing interests**
7

8
479 The authors declare no competing interests.
9

10
11
12
13
14
15
16
17
18
19
20
21
22
23
24
25
26
27
28
29
30
31
32
33
34
35
36
37
38
39
40
41
42
43
44
45
46
47
48
49
50
51
52
53
54
55
56
57
58
59
60
61
62
63
64
65

480 **References**

1
2
481
3
482
5
483
7
484
8
485
10
486
12
487
14
488
16
489
17
490
19
491
21
492
23
493
24
494
26
495
28
496
30
497
32
498
33
499
35
500
37
501
38
502
40
503
42
504
44
505
46
506
47
507
48
49
508
50
509
51
510
53
511
55
56
512
57
58
59
60
61
62
63
64
65

1. AGIP SpA. 1983. Carta magnetica d'Italia. Servizi centrali per l'esplorazione. Met. Appl. Geof., San Donato Milanese.
2. Anderson, H. A. and Jackson J. A. 1987. Active tectonics of the Adriatic region. Geophys. J. R. Astron. Soc., 91, 937–983.
3. Atlas of Geothermal resources in Europe. 2002. Plate 1 of the Heat-Flow density over Europe. European Community Publ. Nr. EUR 17811.
4. Avanzinelli, R., Sapienza, G. T. and Conticelli, S. 2012. The Cretaceous to Paleogene within-plate magmatism of Pachino-Capo Passero (southeastern Sicily) and Adria (La Queglia and Pietre Nere, southern Italy): geochemical and isotopic evidence against a plume-related origin of circum-Mediterranean magmas. Eur. J. Mineral. 24, 73–96. DOI: 10.1127/0935-1221/2012/0024-2185
5. Balogh, K., Colantoni, P., Guerrera, F., Majer, V., Ravasz-Baranyai, L., Renzulli, A., Veneri, F. and Alberini, C. 1994. The Medium-Grained Gabbro of the Jabuka Islet. Scoglio del Pomo, Adriatic Sea. *Giornale di Geologia* 56 (2), 13-25.
6. Bennett, R., Hreinsdottir, S., Buble, G., Basic, T., Bacic, Z., Marjanovic, M., Casale, G., Gendaszek, A. and Cowan, D. 2008. Eocene to present subduction of southern Adria mantle lithosphere beneath the Dinarides. *Geology* 36 (1), 3–6, <http://dx.doi.org/10.1130/G24136A.1>
7. Bernoulli, D. 2007. The pre-Alpine geodynamic evolution of the Southern Alps: A short summary. *Bulletin für angewandte Geologie*, 12(2), 3–10.
8. Boscaini, A., Marzoli, A., Davies, J. F. H. L., Chiaradia, M., Bertrand, H., Zanetti, A., Visonà, D., De Min, A. and Jourdan, F. 2020. Permian post-collisional basic magmatism from Corsica to the Southeastern Alps. *Lithos*, 376-377, 105733, <https://doi.org/10.1016/j.lithos.2020.105733>.
9. Bronner, A., Sauter, D., Manatschal, G., Péron-Pinvidic, G. and Munsch, M. 2011. Magmatic breakup as an explanation for magnetic anomalies at magma-poor rifted margins. *Nature Geoscience* 4, 549-553.
10. Buser, S. 1987. Development of the Dinaric and Julian carbonate platforms and of the intermediate Slovenian basin (NW Yugoslavia). *Memorie della Società Geologica Italiana*, 40, 313–320.
11. Butler, R. W. H., Mazzoli, S., Corrado, S., De Donatis, M., Di Bucci, D., Gambini, R., Naso, G., Nicolai, C., Scrocca, D., Shiner, P. and Zucconi, V. 2004. Applying thick-skinned tectonic models to the Apennine thrust belt of Italy—Limitations and implications. In: K. R. McClay (eds) *Thrust tectonics and hydrocarbon systems: AAPG Memoir 82*, p. 647–667.
12. Calcagnile, G. and Panza, G. F. 1981. The main characteristics of the lithosphere-asthenosphere system in Italy and surrounding regions. *Pure and Applied Geophysics* 119, 865-879.

513
1
514
2
515
3
4
516
5
6
517
7
8
518
9
10
519
11
12
520
13
14
521
15
16
522
17
18
523
19
20
524
21
22
525
23
24
526
25
26
527
27
28
528
29
30
529
31
32
530
33
34
531
35
36
532
37
38
533
39
40
534
41
42
535
43
44
536
45
46
537
47
48
538
49
50
539
51
52
540
53
54
541
55
542
56
543
57
544
58
545
59
546
60
547
61
62
63
64
65

13. Caratori Tontini, F., Stefanelli, P., Giori, I., Faggioni, O. and Carmisciano, c. 2004. The revised aeromagnetic anomaly map of Italy. *Annals of Geophysics* V. 47, N. 5. <https://doi.org/10.4401/ag-3358>

14. Cassetta, F., Ickert, R. B., Mark, D. F., Bonadiman, C., Giacomoni, P. P., Ntaflos, T. and Coltorti, M. 2019. The Alkaline Lamprophyres of the Dolomitic Area (Southern Alps, Italy): Markers of the Late Triassic Change from Orogenic-like to Anorogenic Magmatism. *Journal of Petrology*, 1-36, doi: 10.1093/petrology/egz031.

15. Cassinis, G., Cortesogno, L., Gaggero, L., Perotti, C. R. and Buzzi, L. 2008. Permian to Triassic geodynamic and magmatic evolution of the Brescian Alps (eastern Lombardy, Italy). In G. Cassinis (Ed.), Vol. 127(3). *Stratigraphy and palaeogeography of late- and post-hercynian basins in the Southern Alps, Tuscany and Sardinia (Italy)* (pp. 501–518). Rome: Italian Journal of Geosciences (Bollettino della Societa Geologica Italiana).

16. Cassinis, G., Perotti, C. R. and Ronchi, A. 2012. Permian continental basins in the Southern Alps (Italy) and peri-mediterranean correlations. *International Journal of Earth Sciences (Geologische Rundschau)*, 101, 129–157. <http://dx.doi.org/10.1007/s00531-011-0642-6>.

17. Cazzola, C. and Soudet, H. J. 1993. Facies and Reservoir Characterization of Cretaceous-Eocene Turbidites in the Northern Adriatic. In: Spencer A.M. (eds) *Generation, Accumulation and Production of Europe’s Hydrocarbons III*. Special Publication of the European Association of Petroleum Geoscientists, vol 3. Springer, Berlin, Heidelberg. https://doi.org/10.1007/978-3-642-77859-9_16

18. Chiappini, M., Meloni, A., Boschi, E., Faggioni, O., Beverini, N., Carmisciano, C. and Marson, I. 2000. Shaded relief magnetic anomaly map of Italy and surrounding marine areas. *Annals of Geophysics* 43, 5. <https://doi.org/10.4401/ag-3676>

19. CNR – PFG. 1991. Structural model of Italy and gravity map. *Quaderni della Ricerca Scientifica*, n. 114, vol. 3.

20. D’Agostino, N., Avallone, A., Cheloni, D., D’Anastasio, E., Mantenuto, S. and Selvaggi, G. 2008. Active tectonics of the Adriatic region from GPS and earthquake slip vectors. *Journal of Geophysical Research* 113, doi:10.1029/2008JB005860.

21. Della Vedova, B., Bellani, S., Pellis, G. and Squarci, P. 2001. Deep temperatures and surface heat flow distribution. In: Vai, G.B., Martini, I.P. (Eds.), *Anatomy of an Orogen: The Apennines and Adjacent Mediterranean Basins*. Kluwer Academic Publishers, Dordrecht, The Netherlands, pp. 65–76.

22. Di Bucci, D., Ravaglia, A., Seno, S., Toscani, G., Fracassi, U. and Velinsise G. 2006. Seismotectonics of the southern Apennines and Adriatic foreland: Insights on active regional E-W shear zones from analogue modeling. *Tectonics* 25, TC4015, doi:10.1029/2005TC001898.

548
549
550
551
552
553
554
555
556
557
558
559
560
561
562
563
564
565
566
567
568
569
570
571
572
573
574
575
576
577
578
579
580
581
582
61
62
63
64
65

23. Doglioni, C., Mongelli, F. and Pieri, P. 1994. The Puglia uplift (SE Italy): an anomaly in the foreland of the Apenninic subduction due to buckling of a thick continental lithosphere. *Tectonics* 13, N. 5, doi:10.1029/94TC01501.

24. Eyuboglu, Y., Dudas, F. O., Chatterjee, N., Liu, Z. and Yilmaz-Değerli, S. 2018. Discovery of Latest Cretaceous OIB-type alkaline gabbros in the Eastern Pontides Orogenic Belt, NE Turkey: Evidence for tectonic emplacement of seamounts. *Lithos*, 310-311, 182-200.

25. Faccenna, C., Becker, T. W., Auer, L., Billi, A., Boschi, L., et al. 2014. Mantle dynamics in the Mediterranean. *Review of Geophysics*, 52, 283-332.

26. Fantoni, R. and Franciosi, R. 2010. Tectono-sedimentary setting of the Po Plain and Adriatic Foreland. *Rend. Fis. Acc. Lincei* (2010) 21 (Suppl 1):S197–S209. DOI 10.1007/s12210-010-0102-4

27. Federici, I., Cavazza, W., Okay, A. I., Beyssac, O., Zattin, M., Corrado, S. and Dellisanti, F. 2010. Thermal Evolution of the Permo–Triassic Karakaya Subduction-accretion Complex between the Biga Peninsula and the Tokat Massif (Anatolia). *Turkish Journal of Earth Sciences* 19, 409-429. doi:10.3906/yer-0910-39

28. Fourier, J. 1822. *Théorie analytique de la chaleur*. Paris: Firmin Didot Père et Fils.

29. Frost, B. R., and Shive, P. N. 1986. Magnetic mineralogy of the lower continental crust. *Journal of Geophysical Research*, 91(B6), 6513–6521. <https://doi.org/10.1029/JB091iB06p06513>

30. Gaetani, M. 2010. From Permian to cretaceous: Adria as pivotal between extensions and rotations of Tethys and Atlantic Oceans. In M. Beltrando, A. Peccerillo, M. Mattei, S. Conticelli, & C. Doglioni (Eds.), *The geology of Italy: Tectonics and life along plate margins*. *Journal of the Virtual Explorer*, 36. <http://dx.doi.org/10.3809/jvirtex.2010.00235>. paper no. 6, Electronic Edition.

31. Giori, I., Caratori Tontini, F., Cocchi, L., Carmisciano, C., Bologna, C., Camorali, C., Samarzija, J. And Taylor, P. 2007. The Adriatic Magnetic Anomaly. EGM 2007 International Workshop, Capri – Italy 16-18 april 2007.

32. Handy, M. R., Giese, J., Schmid, S. M., Pleuger, J., Spakman, W., Nuzi, K. and Ustaszewski, K. 2019. Coupled crust-mantle response to slab tearing, bending and rollback along the Dinaride-Hellenide orogen. *Tectonics*, doi:10.1029/2019TC005524.

33. Herak, M. 1986. A new concept of geotectonics of the Dinarides. *Acta Geol.* 16, 1–42.

34. Juračić, M., Novosel, A., Tibljas, D. and Balen, D. 2004. Jabuka shoal, a new location with igneous rocks in the Adriatic Sea. *Geol. Croat.* 57 (1), 81–85.

35. Korbar, T. 2009. Orogenic evolution of the External Dinarides in the NE Adriatic region: a model constrained by tectonostratigraphy of Upper Cretaceous to Paleogene carbonates. *Earth Sci. Rev.* 96, 296–312.

36. Kurevija, T., Vulin, D. and Macenic, M. 2014. Impact of geothermal gradient on ground source heat pump system modeling. *Rudarsko-geološko-naftni zbornik vol 28*, 39-45.

583
584
585
586
587
588
589
590
591
592
593
594
595
596
597
598
599
600
601
602
603
604
605
606
607
608
609
610
611
612
613
614
615
616
617
61
62
63
64
65

37. Le Breton, E., Handy, M.R., Molli, G. and Ustaszewski, K. 2017. Post-20 Ma motion of the Adriatic plate – new constraints from surrounding orogens and implications for crust-mantle decoupling. *Tectonics*, 36, 12, 3135-3154, [10.1002/2016TC004443](https://doi.org/10.1002/2016TC004443)

38. Mancinelli, P., Pauselli, C., Minelli, G. and Federico, C. 2015. Magnetic and gravimetric modeling of the Central Adriatic region. *Journal of Geodynamics* 89, 60-70.

39. Mancinelli, P., Pauselli, C., Minelli, G., Barchi, M. R. and Simpson, G. 2018. Potential evidence for slab detachment from the flexural backstripping of a foredeep: Insight on the evolution of the Pescara basin (Italy). *Terra Nova* 2018, 1-11, DOI: [10.1111/ter.12329](https://doi.org/10.1111/ter.12329).

40. Mancinelli, P., Porreca, M., Pauselli, C., Minelli, G., Barchi, M. R. and Speranza, F. 2019. Gravity and Magnetic Modeling of Central Italy: Insights Into the Depth Extent of the Seismogenic Layer. *Geochemistry, Geophysics, Geosystems*, 20, <https://doi.org/10.1029/2018GC008002>.

41. Mancinelli, P. and Scisciani, V. 2020. Seismic velocity-depth relation in a siliciclastic turbiditic foreland basin: A case study from the Central Adriatic Sea. *Marine and Petroleum Geology* 120, 104554, <https://doi.org/10.1016/j.marpetgeo.2020.104554>.

42. Mancinelli, P., Scisciani, V., Patruno, S. and Minelli, G. 2021. Gravity modeling reveals a Messinian foredeep depocenter beneath the intermontane Fucino Basin (Central Apennines). *Tectonophysics* 821, 229144, <https://doi.org/10.1016/j.tecto.2021.229144>.

43. Mazzeo, F. C., Arienzo, I., Aulinas, M., Casalini, M., Di Renzo, V. and D'Antonio, M. 2018. Mineralogical, geochemical and isotopic characteristics of alkaline mafic igneous rocks from Punta delle Pietre Nere (Gargano, Southern Italy). *Lithos* V. 308–309, 316-328, <https://doi.org/10.1016/j.lithos.2018.03.015>.

44. Menant, A., Angiboust, S. and Gerya, T. 2019. Stress-driven fluid flow controls long-term megathrust strength and deep accretionary dynamics. *Scientific Reports* 9:9714 <https://doi.org/10.1038/s41598-019-46191-y>

45. Menant, A., Angiboust, S., Gerya, T., Lacassin, R., Simoes, M. and Grandin, R. 2020. Transient stripping of subducting slabs controls periodic forearc uplift. *Nature Communications*, 11:1823 <https://doi.org/10.1038/s41467-020-15580-7>

46. Milano, M. and Fedi, M. 2017. Multiscale study of the Adriatic Magnetic Anomaly. EGU Geophysical Research Abstracts Vol. 19, EGU2017-944, EGU General Assembly 2017. <https://meetingorganizer.copernicus.org/EGU2017/EGU2017-944.pdf>

47. Milano, M., Fedi, M. and Fairhead, J. D. 2019. Joint analysis of the magnetic field and total gradient intensity in Central Europe. *Solid Earth* 10, 697-712.

48. Minelli, L., Speranza, F., Nicolosi, I., D'Ajello Caracciolo, F., Carluccio, R., Chiappini, S., et al. 2018. Aeromagnetic investigation of the Central Apennine Seismogenic Zone (Italy): From basins to faults. *Tectonics*, 37, 1435–1453. <https://doi.org/10.1002/2017TC004953>

- 618 49. Moix, P., Beccaletto, L., Kozur, H., Hochard, C., Rosselet, F. and Stampfli G. M. 2008. A new
619 classification of the Turkish terranes and sutures and its implication for the paleotectonic history of
620 the region. *Tectonophysics* 451, 7–39
- 621 50. Moix, P., Vachard, D., Allibon, J., Martini, R., Wernli, R., Kozur, H. W. and Stampfli, G. M. 2013.
622 Palaeotethyan, Neotethyan and Huğlu-Pindos Series in the Lycian Nappes (SW Turkey):
623 Geodynamical Implications. In: Tanner, L.H., Spielmann, J.A. and Lucas, S.G., eds., 2013, *The*
624 *Triassic System. New Mexico Museum of Natural History and Science, Bulletin* 61.
- 625 51. Molli, G., Brogi, A., Caggianelli, A., Capezzuoli, E., Liotta, D., Spina, A. and Zibra, I. 2020. Late
626 Palaeozoic tectonics in Central Mediterranean: a reappraisal. *Swiss Journal of Geosciences*, 113:23,
627 <https://doi.org/10.1186/s00015-020-00375-1>
- 628 52. Montone, P. and Mariucci, M. T. 2015. P-wave Velocity, Density, and Vertical Stress Magnitude
629 Along the Crustal Po Plain (Northern Italy) from Sonic Log Drilling Data. *Pure and Applied*
630 *Geophysics* 172, 6, 1547-1561, DOI 10.1007/s00024-014-1022-5
- 631 53. Montone, P. and Mariucci, M. T. 2020. Constraints on the Structure of the Shallow crust in central
632 italy from Geophysical Log Data. *Scientific Reports* 10:3834 | [https://doi.org/10.1038/s41598-020-](https://doi.org/10.1038/s41598-020-60855-0)
633 [60855-0](https://doi.org/10.1038/s41598-020-60855-0)
- 634 54. Moretti, I. and Royden, L. 1988. Deflection, gravity-anomalies and tectonics of doubly subducted
635 continental lithosphere – Adriatic and Ionian seas. *Tectonics* 7, 875–893.
- 636 55. Nakanishi, A., Kurashimo, E., Tatsumi, Y., et al. 2009. Crustal evolution of the southwestern Kuril
637 Arc, Hokkaido Japan, deduced from seismic velocity and geochemical structure. *Tectonophysics*
638 472, 105–123.
- 639 56. Nicolich, R. 2001. Deep seismic transects. In: Vai, G.B., Martini, I.P. (Eds.), *Anatomy of an Orogen:*
640 *The Apennines and Adjacent Mediterranean Basins. Kluwer Academic Publishers, Dordrecht, The*
641 *Netherlands*, pp. 47–52.
- 642 57. Oldow, J. S., Ferranti, L., Lewis, D. S., Campbell, J. K., D’Argenio, B., Catalano, R., Pappone, G.,
643 Carmignani, L. and Aiken, C. L. V. 2002. Active fragmentation of Adria, the north African
644 promontory, central Mediterranean orogen. *Geology*, 30 (9), 779.
- 645 58. Palinkaš, L. A., Borojević Šošarić, S., Strmić Palinkaš, S., Crnjaković, M., Neubauer, F., Molnár, F.
646 and Bermanec, V. 2010. Volcanoes in the Adriatic Sea: Permo-Triassic magmatism on the Adriatic–
647 Dinaridic carbonate platform. *Acta Mineralogica-Petrographica, Field Guide Series, Vol. 8, PP. 1–15*
- 648 59. Pamić, J. and Balen, D. 2005. Interaction between Permo-Triassic rifting, magmatism and initiation
649 of the Adriatic-Dinaric Carbonate platform (ADCP). *Acta Geol. Hung.* 48 (2), 181–204.
- 650 60. Pauselli, C., Barchi, M. R., Federico, C., Magnani, M. B., and Minelli, G. 2006. The crustal structure
651 of the Northern Apennines (Central Italy): An insight by the CROP03 seismic line. *American Journal*
652 *of Science*, 306(6), 428–450. <https://doi.org/10.2475/06.2006.02>

653
1
654
2
655
3
4
656
5
6
657
7
8
658
9
10
659
11
12
660
13
14
661
15
16
662
17
18
663
19
20
664
21
22
665
23
24
666
25
26
667
27
28
668
29
30
669
31
32
670
33
34
671
35
36
672
37
38
673
39
40
674
41
42
675
43
44
676
45
46
677
47
48
678
49
50
679
51
52
680
53
54
681
55
56
682
57
58
683
59
60
684
61
62
63
64
65

61. Pauselli, C. and Ranalli, G. 2017. Effects of lateral variations of crustal rheology on the occurrence post-orogenic normal faults: The Alto Tiberina Fault (Northern Apennines, Central Italy). *Tectonophysics*, 721, 45–55.

62. Pauselli, C., Gola, G., Mancinelli, P., Trumpy, E., Saccone, M., Manzella, A. and Ranalli G. 2019. A new surface heat flow map of the Northern Apennines between latitudes 42.5 and 44.5 N. *Geothermics* 81, 39-52.

63. Petford, N., Cruden, A.R. and McCaffrey, K.J.W., et al. 2000. Granite magma formation, transport and emplacement in the Earth's crust. *Nature* 408, 669–673.

64. Pullaiah, G., Irving, E., Buchan, K. L. and Dunlop, D. J. 1975. Magnetization changes caused by burial and uplift. *Earth and Planetary Science Letters*, 28, 133–143.

65. Punturo, R., Mamtani, M. A., Fazio, E., Occhipinti, R., Renjith, A. R. and Cirrincione, R. 2017. Seismic and magnetic susceptibility anisotropy of middle-lower continental crust: Insights for their potential relationship from a study of intrusive rocks from the Serre Massif (Calabria, southern Italy). *Tectonophysics*, 712(713), 542–556. <https://doi.org/10.1016/j.tecto.2017.06.020>

66. Radić, D. and Lugović, B. 2004. Petrographic and geochemical correlation between artifacts from the mesolithic layers of Vela Spila and the magmatic rocks of Central Dalmatian Islands. *Dalmacija* 210.7, UDK: 902.66:903.2. https://hrcak.srce.hr/index.php?lang=en&show=clanak&id_clanak_jezik=26610

67. Rochette, P. 1994. Comments on “Anisotropic magnetic susceptibility in the continental lower crust and its implication for the shape of magnetic anomalies”. *Geophysical Research Letters*, 21, 2773–2774.

68. Sassi, F., Mazzoli, C., Merle, R., Brombin, V., Chiaradia, M., Dunkley, D. J. and Marzoli, A. 2020. HT-LP crustal syntectonic anatexis as a source of the Permian magmatism in the Eastern Southern Alps: evidence from xenoliths in the Euganean trachytes (NE Italy). *Journal of the Geological Society*, DOI: <https://doi.org/10.1144/jgs2020-031>.

69. Satolli, S., Speranza, F. and Calamita, F. 2005. Paleomagnetism of the Gran Sasso range salient (central Apennines, Italy): Pattern of orogenic rotations due to translation of a massive carbonate indenter. *Tectonics*, 24, TC4019, doi:10.1029/2004TC001771

70. Scarascia, S., Cassinis, R. and Federici, F. 1998. Gravity modelling of deep structures in the Northern-Central Apennines. *Memorie della Società Geologica Italiana* 52, 231-246.

71. Schlinger, C. M. 1985. Magnetization of lower crust and interpretation of regional magnetic anomalies: Example from Lofoten and Vesterrålen, Norway. *Journal of Geophysical Research*, 90(B13), 11,484–11,504.

72. Schuster, R. and Stüwe, K. 2008. Permian metamorphic event in the Alps. *Geology* 36; no. 8; p. 603–606; doi: 10.1130/G24703A.1.

688
689
690
691
692
693
694
695
696
697
698
699
700
701
702
703
704
705
706
707
708
709
710
711
712
713
714
715
716
717
718
719
720
721
60
61
62
63
64
65

73. Scisciani, V. and Esetime, P. 2017. The Triassic Evaporites in the Evolution of the Adriatic Basin. In: Permo-Triassic salt provinces of Europe, North Africa and the Atlantic Margins. <http://dx.doi.org/10.1016/B978-0-12-809417-4.00024-0>, Elsevier.

74. Scivetti, N., Marcos, P., Pivetta, C. P., Benedini, L., Falco, J. I., Arrouy, M. J., Bahía, M. E., Franzese, J. R. and Gregori, D. A. 2021. Stretching in continental back-arc basins: Insights from subsidence analysis of the Neuquén Basin, Argentina. *Tectonophysics*, 812, 228917.

75. Scrocca, D., Doglioni, C., Innocenti, F., Manetti, P., Mazzotti, A., Bertelli, L., Burbi, L. and D'Offizi, S. (Eds.) 2003. CROP Atlas: seismic reflection profiles of the Italian crust. *Memorie Descrittive della Carta Geologica d'Italia*, 62: pp. 194.

76. Shive, P. N., Blakely, R. J., Frost, B. R., and Fountain, D. M. 1992. Magnetic properties of the lower continental crust. In D. M. Fountain, R. Arculus, & R. W. Kay (Eds.), *Continental lower crust* (pp. 145–177). New York: Elsevier Sci.

77. Speranza, F. and Kissel, C. 1993. First paleomagnetism of Eocene rocks from Gargano: widespread overprint or non rotation? *Geophysical Research Letters* v. 20, n. 23, pages 2627-2630.

78. Stampfli, G.M. and Borel, G.D., 2004. The TRANSMED Transects in Space and Time: constraints on the Paleotectonic Evolution of the Mediterranean Domain. In: Cavazza W., Roure F., Spakman W., Stampfli G.M., Ziegler P.A. (eds) *The TRANSMED Atlas. The Mediterranean Region from Crust to Mantle*. Springer, Berlin, Heidelberg. https://doi.org/10.1007/978-3-642-18919-7_3

79. Stampfli, G. M. and Kozur, H. W. 2006. Europe from the Variscan to the Alpine cycles. In: D.G. Gee and R. Stephenson (Editors), *European lithosphere dynamics*. *Memoir of the Geological Society (London)* 32, 57-82.

80. Stampfli, G. M. and Hochard, C. 2009. Plate tectonics of the Alpine realm. In: Murphy, J.B., Hynes, A.J. and Keppie, J.D., eds, *Ancient orogens and modern analogues*, *Geol. Soc. London Spec. P.*, 327, 89-111.

81. Stampfli G. M., Hochard, C., Vérard, C., Wilhem, C. and von Raumer, J. 2013. The formation of Pangea. *Tectonophysics* 593, 1-19.

82. Stein, S., and Sella, G. 2005. Pleistocene change from convergence to extension in the Apennines as a consequence of Adria microplate motion, in *The Adria Microplate: GPS Geodesy, Tectonics and Hazards*, *Nato Sci. Ser.*, edited by N. Pinter et al., pp. 21–34, Springer, Berlin, Germany.

83. Straub, S. 2003. The evolution of the Izu Bonin - Mariana volcanic arcs (NW Pacific) in terms of major element chemistry. *Geochemistry Geophysics Geosystems*, 4(2), 1018, doi:10.1029/2002GC000357.

84. Šumanovac, F., 2010. Lithosphere structure at the contact of the Adriatic microplate and the Pannonian segment based on the gravity modeling. *Tectonophysics* 485, 94–106.

722
723
724
725
726
727
728
729
730
731
732
733
734
735
736
737
738
739
740
741
742
743
744
745
746
747
748
749
750
751
752
753
754
755
756
61
62
63
64
65

85. Sun, S. -s. and McDonough, W. F. 1989. Chemical and isotopic systematics of oceanic basalts: implications for mantle composition and processes. Geological Society, London, Special Publications 1989, v.42; p. 313-345. doi: 10.1144/GSL.SP.1989.042.01.19

86. Sun, W., Zhao, L., Malusà, M. G., Guillot, S. and Fu, Li-Y. 2019. 3-D Pn tomography reveals continental subduction at the boundaries of the Adriatic microplate in the absence of a precursor oceanic slab. Earth and Planetary Science Letters 510, 131-141.

87. Tari, V., 2002. Evolution of the northern and western Dinarides: a tectonostratigraphic approach. EGU Stephan Mueller Special Publication Series, vol. 1., pp. 223–236.

88. Tassis, G.A., Grigoriadis, V.N., Tziavos, I.N., Tsokas, G.N., Papazachos, C.B. and Vasiljević, I., 2013. A new Bouguer gravity anomaly field for the Adriatic Sea and its application for the study of the crustal and upper mantle structure. Journal of Geodynamics 66, 38–52.

89. Thièblemont, D., Chevremont, P., Castaing, C. and Feybessej, L. 1994. La discrimination géotectonique des roches magmatiques basiques par les éléments traces: réévaluation d'après une base de données et application à la chaîne panafricaine du Togo. Geodinamica Acta, Paris, 7, 3, pp. 139-157.

90. Thybo, H. and Artemieva, I. M. 2013. Moho and magmatic underplating in continental lithosphere. Tectonophysics 609, 605-619.

91. Turcotte, D. L. and Schubert, G. 2002. Geodynamics. Cambridge University Press, Cambridge.

92. Van der Voo, R. 1990. Phanerozoic paleomagnetic poles from Europe and North America and comparisons with continental reconstructions. Reviews of Geophysics 28, 167-206.

93. van Unen, M., Matenco, L., Nader, F. H., Darnault, R., Mandic, O. and Demir, V. 2019. Kinematics of Foreland-Vergent Crustal Accretion: Inferences From the Dinarides Evolution. Tectonics 38, 49–76. <https://doi.org/10.1029/2018TC005066>

94. Vavassis, I., De Bono, A., Stampfli, G. M., Giorgis, D., Valloton, A. and Amelin, Y. 2000. U-Pb and Ar-Ar geochronological data from the Pelagonian basement in Evia (Greece): geodynamic implications for the evolution of Paleotethys. Schweizerische Mineralogische und Petrographische Mitteilungen 80: 21-43.

95. Velić, I., Vlahović, I. and Matičec, D. 2002. Depositional sequences and palaeogeography of the Adriatic carbonate platform. Memorie della Società Geologica Italiana, 57, 141–151.

96. Viandante, M. G., Calamita, F., Di Vincenzo, M. and Tavarnelli, E. 2006. Il sistema a pieghe e sovrascorrimenti del Gran Sasso d'Italia nella culminazione assiale della catena pliocenico-aternaria centro-Appenninica. Rendiconti della Società Geologica Italiana, 2, Nuova Serie, 187-190

97. Wasilewski, P. J., Thomas, H. H., and Mayhew, M. A. 1979. The Moho as a magnetic boundary. Geophysical Research Letters, 6(7), 544–541

757
1
758
2
759
3
4
760
5
6
761
7
8
762
9
10
763
11
12
764
13
14
765
15
16
766
17
18
19
20
21
22
23
24
25
26
27
28
29
30
31
32
33
34
35
36
37
38
39
40
41
42
43
44
45
46
47
48
49
50
51
52
53
54
55
56
57
58
59
60
61
62
63
64
65

98. Wasilewski, P. J., and Mayhew, M. A. 1992. The Moho as a magnetic boundary revisited. Geophysical Research Letters, 19(22), 2259–2262.

99. Watts, A. B. 2001. Isostasy and flexure of the lithosphere. Cambridge University Press, Cambridge.

100. Werner, R., Baranov, B., Hoernle, K., van den Bogaard, P., Hauff, F. and Tararin, I. 2020. Discovery of Ancient Volcanoes in the Okhotsk Sea(Russia): New Constraints on the Opening History of the Kurile Back Arc Basin. Geosciences, 2020, 10, 442; doi:10.3390/geosciences10110442

101. Zandt, G., Myers, S. C. and Wallace, T. C. 1995. Crust and mantle structure across the Basin and Range – Colorado Plateau boundary at 37°N latitude and implications for Cenozoic extensional mechanism. Journal of Geophysical Research 100, NO. B6, 10529 doi: 10.1029/94JB03063